Volume 13
Number 19
21 May 2022
Pages 2707-2872

Polymer Chemistry

rsc.li/polymers

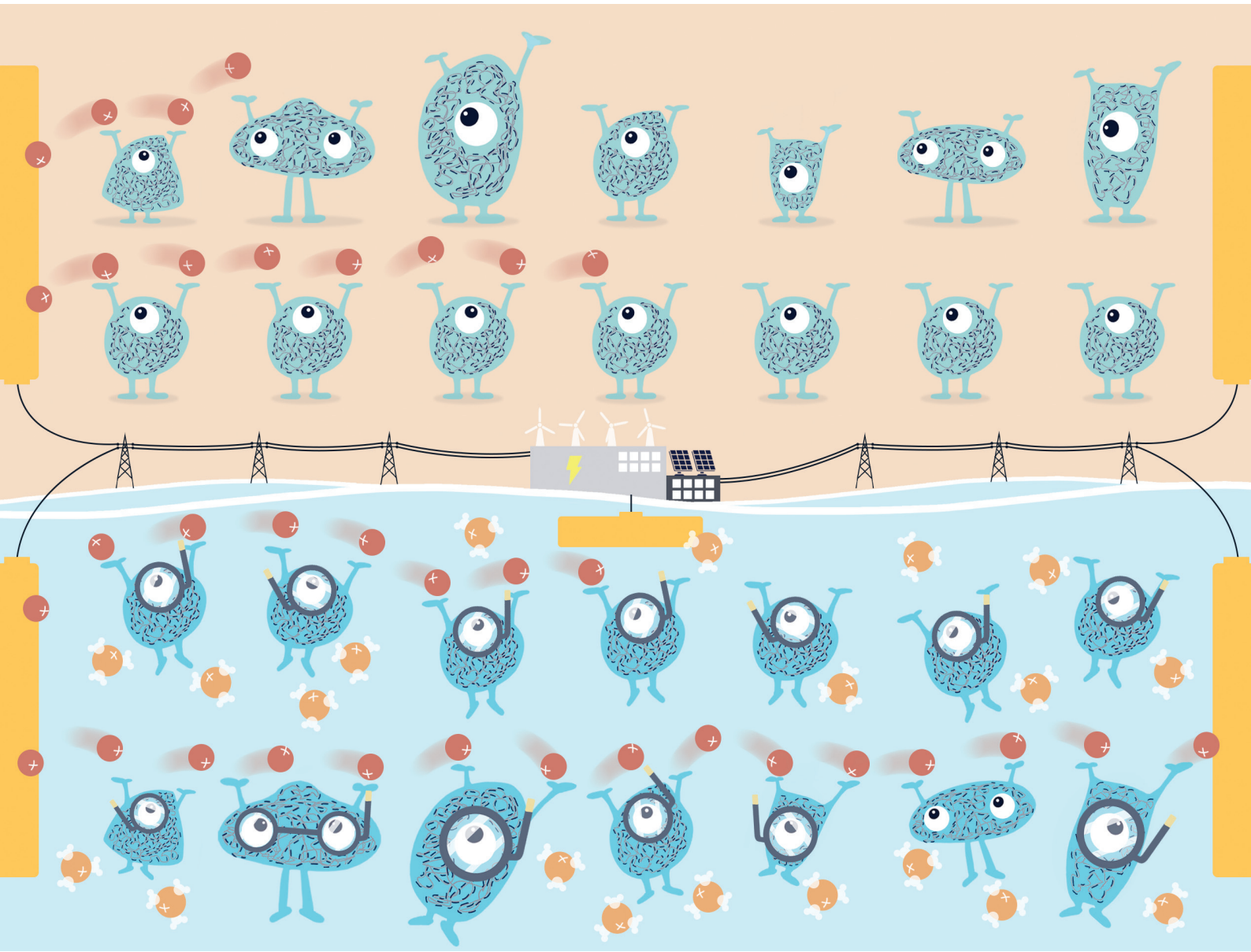

ISSN 1759-9962

ROYAL SOCIETY OF CHEMISTRY

PAPER
Laure V. Kayser *et al.*
Influence of the molecular weight and size distribution of PSS on mixed ionic-electronic transport in PEDOT:PSS

Polymer Chemistry

ROYAL SOCIETY OF CHEMISTRY

PAPER

View Article Online
View Journal | View Issue

Cite this: *Polym. Chem.*, 2022, **13**, 2764

Influence of the molecular weight and size distribution of PSS on mixed ionic-electronic transport in PEDOT:PSS†

Chun-Yuan Lo,[a] Yuhang Wu,[b] Elorm Awuyah,[a] Dilara Meli,[c] Dan My Nguyen,[a] Ruiheng Wu,[d] Bohan Xu,[c] Joseph Strzalka,[e] Jonathan Rivnay,[f,g] David C. Martin[b,h] and Laure V. Kayser *[a,b]

The commercially available polyelectrolyte complex poly(3,4-ethylenedioxythiophene):poly(styrene sulfonate) (PEDOT:PSS) is ubiquitous in organic and hybrid electronics. As such, it has often been used as a benchmark material for fundamental studies and the development of new electronic devices. Yet, most studies on PEDOT:PSS have focused on its electronic conductivity in dry environments, with less consideration given to its ion transport, coupled ionic-electronic transport, and charge storage properties in aqueous environments. These properties are essential for applications in bioelectronics (sensors, actuators), charge storage devices, and electrochromic displays. Importantly, past studies on mixed ionic-electronic transport in PEDOT:PSS neglected to consider how the molecular structure of PSS affects mixed ionic-electronic transport. Herein, we therefore investigated the effect of the molecular weight and size distribution of PSS on the electronic properties and morphology of PEDOT:PSS both in dry and aqueous environments, and overall performance in organic electrochemical transistors (OECTs). Using reversible addition–fragmentation chain transfer (RAFT) polymerization with two different chain transfer agents, six PSS samples with monomodal, narrow ($Đ$ = 1.1) and broad ($Đ$ = 1.7) size distributions and varying molecular weights were synthesized and used as matrices for PEDOT. We found that using higher molecular weight of PSS (M_n = 145 kg mol^{-1}) and broad dispersity led to OECTs with the highest transconductance (up to 16 mS) and [μC^*] values (~140 F cm^{-1} V^{-1} s^{-1}) in PEDOT:PSS, despite having a lower volumetric capacitance (C^* = 35 ± 4 F cm^{-3}). The differences were best explained by studying the microstructure of the films by atomic force microscopy (AFM). We found that heterogeneities in the PEDOT:PSS films (interconnected and large PEDOT- and PSS-rich domains) obtained from high molecular weight and high dispersity PSS led to higher charge mobility (μ_{OECT} ~ 4 cm^2 V^{-1} s^{-1}) and hence transconductance. These studies highlight the importance of considering molecular weight and size distribution in organic mixed ionic-electronic conductor, and could pave the way to designing high performance organic electronics for biological interfaces.

Received 28th February 2022,
Accepted 21st March 2022

DOI: 10.1039/d2py00271j

rsc.li/polymers

Introduction

The polyelectrolyte complex of poly(3,4-ethylenedioxythiophene) and poly(styrene sulfonate) (PEDOT:PSS) is one of the most commonly used organic conductors because of its high electrical conductivity (over 1000 S cm^{-1} upon secondary doping) and stability as a water dispersion.[1,2] Since being first reported in 1988,[3] PEDOT:PSS has been used in a large range of electronic applications including antistatic coatings,[4] hole-conducting interlayers,[5,6] transparent electrodes,[2,7] and thermoelectric materials.[8] These applications mostly rely on the electronic conductivity of PEDOT:PSS. But, PEDOT:PSS is also a mixed ionic-electronic conductor: it can transport both electronic charges (holes) and ions, and exhibits charge storage and coupled transport properties. These properties expand the

[a]*Department of Chemistry and Biochemistry, University of Delaware, Newark, Delaware, 19716, USA. E-mail: lkayser@udel.edu*
[b]*Department of Materials Science and Engineering, University of Delaware, Newark, Delaware, 19716, USA*
[c]*Department of Materials Science and Engineering, Northwestern University, Evanston, Illinois 60208, USA*
[d]*Department of Chemistry, Northwestern University, Evanston, Illinois 60208, USA*
[e]*X-Ray Science Division, Argonne National Laboratory, Lemont, Illinois 60611, USA*
[f]*Department of Biomedical Engineering, Northwestern University, Evanston, Illinois 60208, USA*
[g]*Simpson Querrey Institute, Northwestern University, Chicago, Illinois 60611, USA*
[h]*Department of Biomedical Engineering, University of Delaware, Newark, Delaware, 19716, USA*

† Electronic supplementary information (ESI) available. See DOI: https://doi.org/10.1039/d2py00271j

utility of PEDOT:PSS to applications where both transport mechanisms are necessary such as in batteries[9] and supercapacitors,[10] light-emitting electrochemical cells,[11] electrochromic windows,[12] actuators,[13] chemical,[14] biological sensors,[15] and organic electrochemical transistors (OECTs)[16] for sensing and neuromorphic computing.[17,18]

For most applications, a commercial formulation of PEDOT:PSS is used (*e.g.*, CleviosTM PH 1000, a high conductivity formulation commercialized by Heraeus) to which additives are used to achieve the desired electronic properties. These additives include high boiling, polar solvents such as dimethyl sulfoxide (DMSO),[19,20] surfactants such as Triton X-100,[21,22] and sulfuric acid[23–25] which effectively enhance the electronic conductivity.[26–29] This enhancement, also coined secondary doping, is primarily due to changes in the film morphology of PEDOT:PSS. Without additives, PEDOT:PSS films exhibit PEDOT:PSS rich domains dispersed in a PSS matrix.[30] With additives, the morphology changes to a more fibrillar microstructure, with more closely interconnected PEDOT domains that facilitate hole transport. Studies have also found that the morphology, and therefore electronic conductivity, is also related to the molecular structure of PEDOT:PSS. Fan *et al.* compared two commercial formulations of PEDOT:PSS, Clevios P and Clevios PH 1000.[31] They found that the conductivity of PH 1000 was approximately one order of magnitude higher than Clevios P after secondary doping. Based on the size distribution of PEDOT:PSS gel particles in solution, the authors hypothesized that this increase in conductivity was due to the higher molecular weight of PEDOT in PH 1000. What leads to this higher molecular weight PEDOT, however, was not clear and has not been disclosed by the manufacturer. A possible explanation could be that a higher molecular weight of PSS results in the formation of larger gel particles of PEDOT:PSS, and potentially higher molecular weight of PEDOT. However, Kim *et al.* found that PSS samples synthesized by atom-transfer radical polymerization (ATRP) at lower molecular weights led to PEDOT:PSS films with higher conductivities (422 S cm^{-1} for PSS with M_n = 33 kg mol^{-1}, $Đ$ = 1.21, *versus* 325 S cm^{-1} for M_n = 58 kg mol^{-1}, $Đ$ = 1.65).[32] A similar trend was observed for PSS synthesized by free radical polymerization with a multimodal size distribution and Đ over 2.3. Interestingly, the PSS samples with low dispersity, synthesized by ATRP, resulted in higher conductivity for PEDOT:PSS (15–30% increase) due to higher degrees of film crystallinity. Overall, it remains unclear how the molecular weight and distribution of PSS is connected to that PEDOT. But, these past studies highlight the importance of controlling the molecular structure and film morphology of PEDOT:PSS to achieve high electrical conductivity.

While the connection between molecular structure, film morphology, and electrical conductivity of PEDOT:PSS has been extensively studied,[26] similar structure–property relationships for mixed ionic-electronic transport remain relatively underexplored. Rivnay *et al.* studied the effect of ethylene glycol (EG) additives on commercial PEDOT:PSS. This additive, however, led to a significant decrease in the ionic mobility and a loss of performance in OECT devices with over 10% of EG.[33] They also investigated the influence of crystallinity and composition of PEDOT:PSS films. Post-treatment with sulfuric acid of PEDOT:PSS enhanced the crystallinity and nanoporosity and led to 3.6 times larger volumetric capacitance (113 F cm^{-3}) than PEDOT:PSS film with the addition of EG.[34] Mecerreyes *et al.* introduced divinylsulfone as a crosslinker for commercial PEDOT:PSS to improve the transconductance value and stability in OECT devices.[35] An understanding of the interplay between electronic transport, ionic transport, and ionic-electronic coupling, as they relate to film morphology, is therefore necessary to optimize device performance. All studies on mixed transport in PEDOT:PSS, however, have been conducted on its commercial form for which important molecular parameters, such as molecular weight and dispersity of PSS, are not disclosed. As previously discussed, these molecular parameters have strong effects on the electrical conductivity and film morphology. As such, we hypothesized that they are also important to consider for applications where PEDOT:PSS is used as a mixed ionic-electronic conductor.

Herein, we study the effect of the molecular weight and size distribution of PSS on mixed ionic-electronic transport in PEDOT:PSS and OECT performance. Using reversible addition–fragmentation chain transfer (RAFT) polymerization, we synthesized a series of PSS with varying molecular weights, with both narrow and broad size distributions by careful choice of the chain transfer agent. This approach, inspired by the work of Anastasaki and coworkers with polystyrene,[36] provides a simple strategy to precisely synthesize PSS with varying molecular weights while maintaining a monomodal size distribution. We studied the effect of the molecular weight and dispersity of PSS on the electronic conductivity (with and without secondary doping) of PEDOT:PSS, its volumetric capacitance, impedance behavior, and performance and stability in OECTs. To establish structure–property relationships, we determined the film composition and morphology by X-ray photoelectron spectroscopy (XPS), grazing-incidence wide-angle X-ray scattering (GIWAXS), and atomic force microscopy (AFM). We found that, unlike in previous studies,[32] the dispersity of PSS (monomodal size distribution) had little effect on the electrical conductivity under dry conditions. However, heterogeneities in the PEDOT:PSS films at high dispersity of PSS are responsible for their superior OECT performance in the presence of an electrolyte. Our study highlights the importance of considering the molecular structure of PSS to control the morphology of PEDOT:PSS, and ultimately enhance mixed ionic-electronic transport.

Results and discussion

Polymerization of PSS with narrow and broad dispersity using different RAFT chain transfer agents and preparation of PEDOT:PSS

To study the effect of the molecular weight and size distribution of PSS on the properties of PEDOT:PSS, we first needed

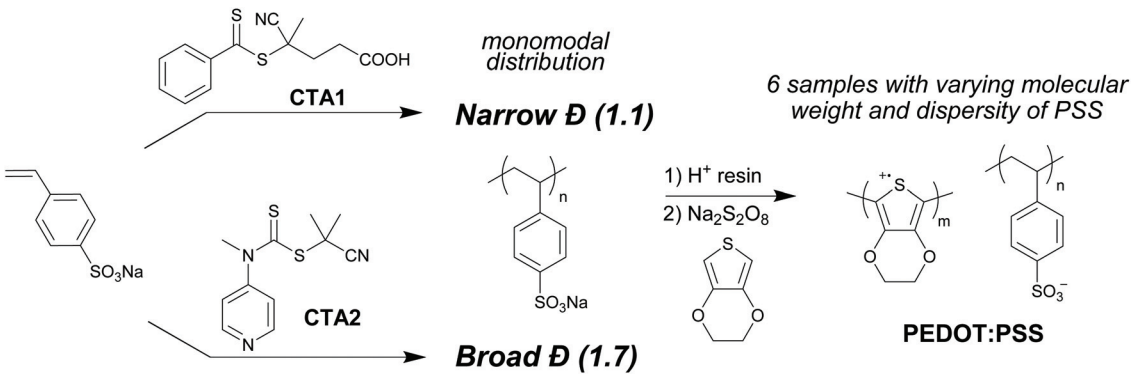

Scheme 1 Synthesis of PEDOT:PSS from poly(styrene sulfonate) with varying molecular weight and size distribution prepared by RAFT polymerization.

to establish a synthetic approach that would allow us to precisely control each parameter without affecting the shape of the distribution. As the shape of the molecular weight distribution has been previously shown to affect the rheological and mechanical properties of polymers,[40] we decided to focus our efforts on monomodal distributions. To obtain narrow and monomodal $Đ$ of PSS, controlled radical polymerizations such as RAFT and atom transfer radical polymerization (ATRP)[37,38] of sodium styrene sulfonate (NaSS) under aqueous conditions have been well-established.[39] In particular, the chain transfer agent **CTA1** (Scheme 1) under RAFT polymerization conditions was previously shown to lead to dispersity around 1.1.[39,41] Using **CTA1**, we synthesized PSSNa with three different molecular weights (33, 58, and 145 kg mol^{-1}) and narrow dispersity ($Đ$ = 1.1) as confirmed by size exclusion chromatography (SEC) (Table 1 and Fig. 1).

To obtain PSS with a broad molecular weight distribution while maintaining a monomodal shape, however, is more challenging. The use of a conventional free radical polymerization leads to a broad dispersity ($Đ$ = 2.3), but the SEC trace is clearly multimodal.[32] Whitfield *et al.* previously showed that the molecular weight distribution of polystyrene can remain monomodal and be precisely tuned from low to high dispersity (~1.1 to 2.1) by mixing RAFT chain transfer agents with different chain-transfer activity.[36] In particular, when **CTA2** (Scheme 1) was used as the sole chain-transfer agent, a dispersity of 2.1 was obtained for polystyrene. The presence of pyridine on **CTA2** deactivated the C=S bond thereby destabilizing the radical intermediate. Thus, **CTA2** leads to a poor control over the polymerization with highly activated monomers such as styrene and high dispersity of the molecular weight distribution.[38,42] We therefore evaluated the use of **CTA2** to obtain PSSNa with a broad dispersity. When high molecular weights were targeted (58 and 145 kg mol^{-1}), the use of 100% **CTA2** resulted in the formation of PSSNa with $Đ$ = 1.7 (**PSS 58k-1.7** and **PSS 144k-1.7**) (Fig. 1b and c). At lower targeted molecular weights, however, a bimodal distribution was obtained with a much broader dispersity than expected (**PSS 35k-2.3**, Fig. 1a). To address this problem, we used a 1 : 1 mixture of **CTA1** and **CTA2**. By using this combination of chain-transfer agents, **PSS 32k-1.7** was obtained with a monomodal size distribution shape and a broader dispersity ($Đ$ = 1.7) than **PSS 33k-1.1** (Fig. 1a). As shown in Fig. 1, we were able to prepare PSS samples with well controlled molecular weights and monomodal size distributions. Importantly, the maxima of the distributions and number average molecular weight remain the same for the narrow and broad dispersity samples. This level of control over PSS allows us to directly study the effect of PSS dispersity on mixed ionic-electronic transport in PEDOT:PSS. Six different samples of PEDOT:PSS were therefore pre-

Table 1 Summary of sodium poly(styrene sulfonate) polymers obtained by RAFT polymerization

Polymer[a]	RAFT CTA	[RAFT] : [M] : [I]	Time (h)	Conv.[b] (%)	$M_{n,theor}$ [b] (kg mol^{-1})	$M_{n,exp}$ [c] (kg mol^{-1})	$M_{w,exp}$ [c] (kg mol^{-1})	$Đ$
PSS 33k-1.1	CTA1	1 : 190 : 0.2	16	90	34.9	33.7	38.1	1.1
PSS 35k-2.3	CTA2	1 : 187 : 0.2	24	83	31.9	35.4	82.5	2.3[d]
PSS 32k-1.7	CTA1 + 2	1 : 155 : 0.2[e]	24	97	31.2	31.7	52.6	1.7[e]
PSS 58k-1.1	CTA1	1 : 316 : 0.2	24	90	58.9	58.0	62.0	1.1
PSS 58k-1.7	CTA2	1 : 260 : 0.2	36	97	52.3	57.8	100.7	1.7
PSS 145k-1.1	CTA1	1 : 710 : 0.2	24	95	138.9	145.5	166.9	1.1
PSS 144k-1.7	CTA2	1 : 730 : 0.3	48	99	150.6	144.2	243.2	1.7

[a] Example for **PSS 33k-1.1** of the naming convention used in this article: 33k refers to 33 kg mol^{-1}, the number average molecular weight of the PSSNa polymer and 1.1 refers to the $Đ$. [b] Obtained by ^{1}H NMR in D_2O. [c] Obtained by size exclusion chromatography (SEC) in water buffer : methanol 80 : 20 calibrated against PSSNa standards using a refractive index detector. [d] Exhibits a shoulder at low molecular weights. [e] Monomodal distribution obtained by mixing **CTA1** and **CTA2** in a 1 : 1 ratio.

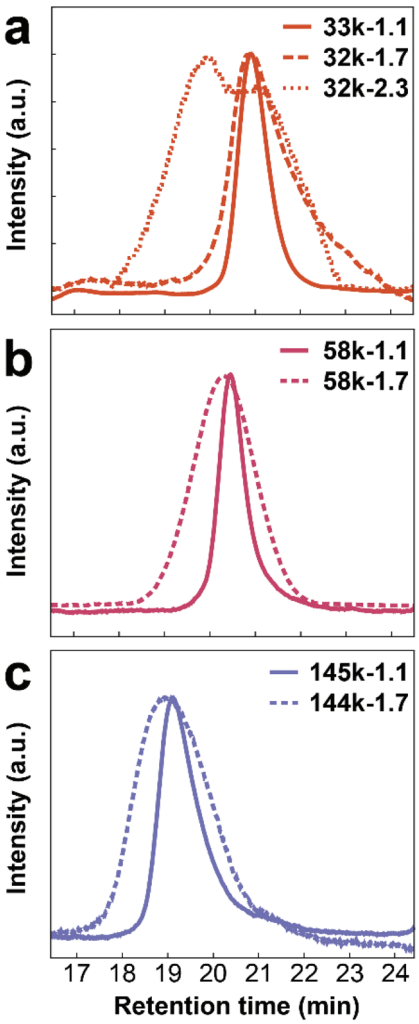

Fig. 1 SEC traces of PSS prepared by RAFT polymerization with **CTA1** (narrow $Đ$) and **CTA2** (broad $Đ$). (a) M_n = 33 kg mol^{-1}, (b) M_n = 58 kg mol^{-1}, and (c) M_n = 145 kg mol^{-1}.

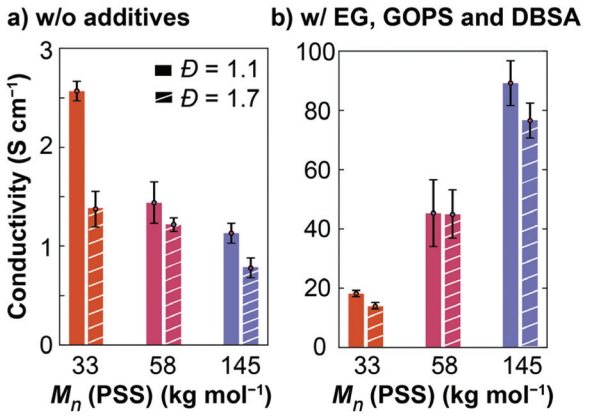

Fig. 2 Effect of the molecular weight and dispersity of PSS on the electrical conductivity of PEDOT:PSS as measured by four-point probe. (a) Neat PEDOT:PSS. (b) With 5 vol% EG, 1 vol% GOPS, and 0.1 vol% DBSA. Error bars correspond to the standard deviation from the average of three independently-synthesized samples.

pared from these PSS polymers, with a monomodal distribution, using an established oxidative polymerization procedure (Scheme 1).

Electronic conductivity of PEDOT:PSS as a function of PSS molecular weight and dispersity

Prior to studying the mixed ionic-electronic properties of these six PEDOT:PSS samples in a wet environment, we investigated their electronic conductivity under dry conditions using a four-point probe. As seen in Fig. 2a and S2a,† a lower molecular weight and lower dispersity (**PEDOT:PSS 33k-1.1**) results in the highest conductivity (2.6 ± 0.1 S cm^{-1}) when PEDOT:PSS is spin-coated neat (without secondary additives). The conductivity decreases to 1.4 ± 0.2 S cm^{-1} and 1.1 ± 0.1 S cm^{-1} when PSS is 58 kg mol^{-1}and 145 kg mol^{-1} (low dispersity), respectively. Only a small effect of the dispersity was observed. In general, when no secondary dopant was used, the conductivity was slightly lower when PSS had a dispersity of 1.7 instead of $Đ$ = 1.1. These observations are consistent with previous reports on the effect of dispersity of PSS on the conductivity of PEDOT:PSS.[32] This effect was most noticeable for lower molecular weight PSS (33 kg mol^{-1}), as the conductivity was almost doubled in the low dispersity sample.

As PEDOT:PSS is most often used in the presence of additives and co-solvents, we then studied the same materials with additives relevant to applications in mixed ionic-electronic conductors. To the PEDOT:PSS dispersions in water, 5 vol% ethylene glycol (EG), 1 vol% (3-glycidyloxypropyl)trimethoxysilane (GOPS), and 0.1 vol% dodecylbenzenesulfonic acid (DBSA) were added, a combination often used for OECT studies.[43–45] Interestingly, we found a reverse trend for the effect of molecular weight on the conductivity compared with the neat samples (Fig. 2b and S2b†). The electrical conductivity of PEDOT:PSS, with these additives, increased from 18 ± 1.1 S cm^{-1} to 90 ± 7.6 S cm^{-1} when PSS increases from 33 to 145 kg mol^{-1}. In the presence of additives, however, changing the dispersity of PSS only had a small effect on the electronic conductivity. We found that the conductivity was slightly lower or within error in samples with a broad PSS distribution. From these experiments, we can therefore conclude that the secondary doping effect of PEDOT:PSS outweighs the PSS dispersity considerations (for monomodal distributions), but molecular weight is an important factor to consider for electronic conductivity under dry conditions. In the following sections, we study the electronic properties of PEDOT:PSS under aqueous conditions with these same additives. In particular, GOPS is necessary as a crosslinker to avoid the re-dispersion of PEDOT:PSS in water.

Effect of PSS molecular weight and dispersity on the volumetric capacitance and impedance of PEDOT:PSS

Next, we studied the electrochemical behavior of PEDOT:PSS in the presence of an aqueous electrolyte as a function of the molecular weight and dispersity of PSS. To determine the volu-

metric capacitance (C^*), a measure of the strength of the ionic-electronic coupling, we performed cyclic voltammetry (CV) on all the PEDOT:PSS samples at various film thicknesses (Fig. S3†). The voltammograms all display a quasi-rectangular shape, similar to commercial PEDOT:PSS, indicative of a capacitive charge storage.[46,47] To determine the volumetric capacitance for each PEDOT:PSS sample, the following equation[48] was used:

$$C^* = \frac{\int_{E_s}^{E_f} I(E)\mathrm{d}E}{2V(E_f - E_s)v} \quad (1)$$

In eqn (1), E_f and E_s are the finishing and starting potential in the CV scans, respectively. $I(E)$ is the instantaneous current. V and v are used to represent the volume (WdL_t) of the spin-coated PEDOT:PSS thin films and the scan rate (0.1 V s^{-1}), respectively. The volumetric capacitance obtained for each PEDOT:PSS sample with varying molecular weights and dispersity are presented in Fig. 3. At low dispersity of PSS ($Đ$ = 1.1), the volumetric capacitance slightly increases with the molecular weight of PSS: from 41 ± 6.5 F cm^{-3} (**PEDOT:PSS 33k-1.1**) to 48 ± 7.1 F cm^{-3} (**PEDOT:PSS 145k-1.1**). At higher dispersity of PSS ($Đ$ = 1.7), no clear trend as a function of molecular was observed. However, at identical molecular weight of PSS, the higher dispersity samples all showed a lower volumetric capacitance than the low dispersity ones. This effect is particularly significant at high molecular weights of PSS (145 kg mol^{-1}) where C^* drops to 31 ± 5.5 F cm^{-3} when $Đ$ = 1.7. To summarize, having a higher molecular weight and low dispersity of PSS lead to a higher charge storage capacitance in PEDOT:PSS (48 ± 7.1 F cm^{-3}), even slightly higher than the C^* for Clevios PH 1000 (~ 39 F cm^{-3}) with identical additives reported by Rivnay *et al.*[49,50] PEDOT:PSS samples prepared from broad dispersity PSS have volumetric capacitance values below those of the commercial sample, whereas the narrow dispersity samples provide values slightly above average. These results suggest that the molecular weight of PSS has little influence on the charge storage capacitance of PEDOT:PSS, while having a lower dispersity leads to an increase in C^* due to a more efficient ionic-electronic coupling.

To gain further insights into the electrochemical behavior of PEDOT:PSS, we performed electrochemical impedance spectroscopy (EIS) on all the samples. The impedance amplitudes of all samples are presented in Fig. S4.† As expected, all PEDOT:PSS samples have a significantly lower impedance than the bare gold electrode.[50,51] Similar impedance behaviors are observed for all the samples, with minimal deviations in the high- and low-frequency regimes, which could possibly be due to differences in contact resistance and capacitance, respectively.[34,50–52] The Nyquist and Bode plots of all the samples are also similar (representative Nyquist and Bode plots for PEDOT:PSS at each molecular weight and dispersity of PSS are shown in Fig. 4 and S4,† respectively). The EIS data was fitted to an equivalent circuit model (Fig. 4 inset), including a simplified Randle's circuit and a generalized finite-length Warburg element. This equivalent circuit model has been previously reported for commercial PEDOT:PSS, and the low χ^2 values (<0.01) for all samples suggest that the proposed model accurately describes the behavior of our PEDOT:PSS samples.[53–55] The elements present in the model consist of R_s, the solution and contact resistance, C_d, the double-layer capacitance, and R_c the charge transfer resistance. In addition, as the slope of data points in the low-frequency regime is larger than 1, a generalized finite length Warburg element (Z_o) was selected for simulating ion diffusion into the PEDOT:PSS films.[56] The tabulated values for these elements for representative samples are tabulated in Table S1.† By normalizing the values for the Warburg element for geometric factors in the low frequency regime (0.1 Hz), where capacitance dominates

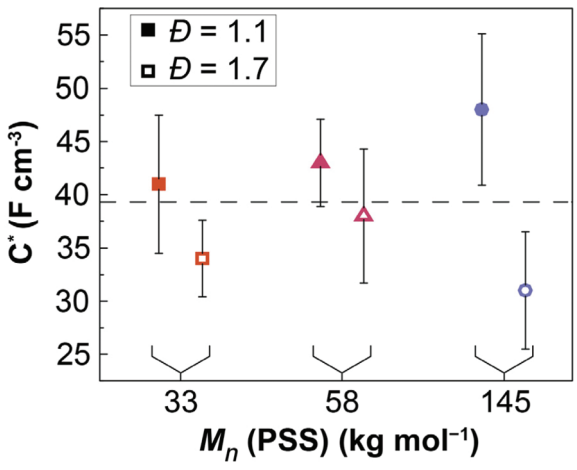

Fig. 3 Volumetric capacitance (C^*) of PEDOT:PSS samples as a function of the molecular weight and dispersity of PSS. The error bars represent the standard deviation from the average value of four independently prepared samples. The dashed line represents the C^* of commercial PEDOT:PSS (Clevios PH 1000) as reported by Rivnay *et al.*[49]

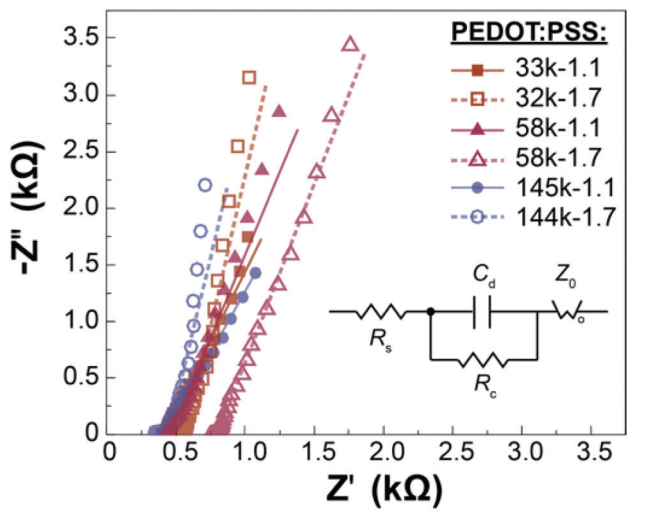

Fig. 4 Representative Nyquist plots for PEDOT:PSS samples with varying molecular weight and dispersity of PSS (symbols: data from measurements; lines: fitted data from the equivalent circuit model shown in the inset).

the impedance behavior, we can estimate the trends in capacitance behavior as a function of PSS molecular weight and dispersity (Fig. S5†). We found similar trends in the capacitance by EIS as with our CV studies, which further validates our EIS studies.

Effect of PSS molecular weight and dispersity on the performance of PEDOT:PSS in OECT

As shown above, the molecular weight and dispersity of PSS affect the conductivity and the volumetric capacitance of PEDOT:PSS. These properties are directly related to the transconductance (g_m), a figure of merit of organic electrochemical transistors (OECTs).[34,57,58] As such, we were interested in evaluating the influence of the molecular parameters of PSS on the performance of PEDOT:PSS in OECTs. To narrow the molecular design space, we chose to focus only on the three samples which showed the strongest differences in conductivity and volumetric capacitance: (1) a low molecular weight and low dispersity PSS (**PEDOT:PSS 33k-1.1**), (2) a high molecular weight and low dispersity PSS (**PEDOT:PSS 145k-1.1**), and (3) a high molecular weight and high dispersity PSS (**PEDOT:PSS 144k-1.7**). OECT devices were fabricated with varying PEDOT:PSS channel dimensions (W, d, L_C) from these three samples (Fig. S1†), and output and transfer curves were collected. Examples for these curves are shown in Fig. 5a and b, respectively, for **PEDOT:PSS 145k-1.1**. These OECT devices, similar to commercial PEDOT:PSS, operate in depletion mode as seen by the decrease in drain current (I_D) with increasing gate voltages (V_G).[59] As previously described, the peak transconductance (g_m) scales linearly with WdL_C^{-1} ($V_{Th} - V_G$).[49] We therefore plotted the g_m of the selected PEDOT:PSS samples with varying film thickness and channel width samples as a function of WdL_C^{-1} ($V_{Th} - V_G$) (Fig. 5c). Each PEDOT:PSS sample follows this linear trend ($R^2 > 0.9$) with the slope of the fitting line representing the product of the mobility and volumetric capacitance [μC^*], a figure of merit for mixed ionic-electronic conductors.[60] The values of g_m, [μC^*], and μ_{OECT} measured and calculated from these device studies are tabulated in Table S2.† The nearly overlapped fitted lines of **PEDOT:PSS 33k-1.1** and **PEDOT:PSS 145k-1.1** imply that for an identical dispersity ($Đ = 1.1$), the molecular weight of PSS does not influence the OECT performance. Their [μC^*] are identical within error at 31.7 ± 13.9 and 32.2 ± 6.8 F cm^{-1} V^{-1} s^{-1}, respectively. However, because C^* was slightly lower for **PEDOT:PSS 33k-1.1**, its μ_{OECT} is slightly higher, up to 1.17 cm^2 V^{-1} s^{-1} *versus* 0.92 cm^2 V^{-1} s^{-1} for **PEDOT:PSS 145k-1.1**. Conversely, the dispersity of the PSS has a strong influence on performance. We found that **PEDOT:PSS 144k-1.7** exhibits the highest OECT performance with transconductance values up to 16.1 mS and [μC^*] of 142.4 ± 27.3 F cm^{-1} V^{-1} s^{-1}, over 4 times higher than those of a low dispersity sample of identical molecular weight. This result is particularly surprising because **PEDOT:PSS 144k-1.7** had the lowest volumetric capacitance (C^*) of all samples. By calculating μ_{OECT}, we found that this low capacitance is compensated by a ~ 6 times higher charge mobility in high dispersity PSS (μ_{OECT} ~ 4.17 *vs.* 0.77 cm^2 V^{-1} s^{-1}). Overall, we found that higher molecular weight and dispersity of PSS in PEDOT:PSS samples leads to enhanced mixed ionic-electronic transport. Unlike previous reports on the effect of the size distribution of PSS on the electronic properties of PEDOT:PSS in a dry state,[32] we found that a broad distribution of PSS is necessary to promote higher charge mobility under hydrated conditions, but has a detrimental effect on the ionic-electronic coupling (*i.e.*, decreased volumetric capacitance).

To rationalize these findings, we characterized the PEDOT:PSS films for their composition and morphology. First, to explain the differences in electrical conductivity observed in the dry state as a function of molecular weight, we used X-ray photoelectron spectroscopy (XPS) to determine the film composition, in particular the surface ratio of PSS to PEDOT. While all the PEDOT:PSS samples were prepared using the same PSS/PEDOT molar ratio (1.9), differences in surface composition were observed by XPS. As previously established,[61] the PSS/PEDOT ratio can be determined by analyzing the S(2p) signals on the XPS. Signals between 167 and 172 eV are indicative of the sulfur binding energy in PSS while those between 162 and 167 eV are attributed to the sulfur in PEDOT (Fig. 6a).[62] The area ratio of the S(2p) peaks can therefore be used to estimate the relative composition of PSS to PEDOT at the surface.[63] We studied the PSS/PEDOT ratio of all six PEDOT:PSS samples with varying molecular weight and dispersity of PSS (Fig. 6b). We focused our studies on PEDOT:PSS

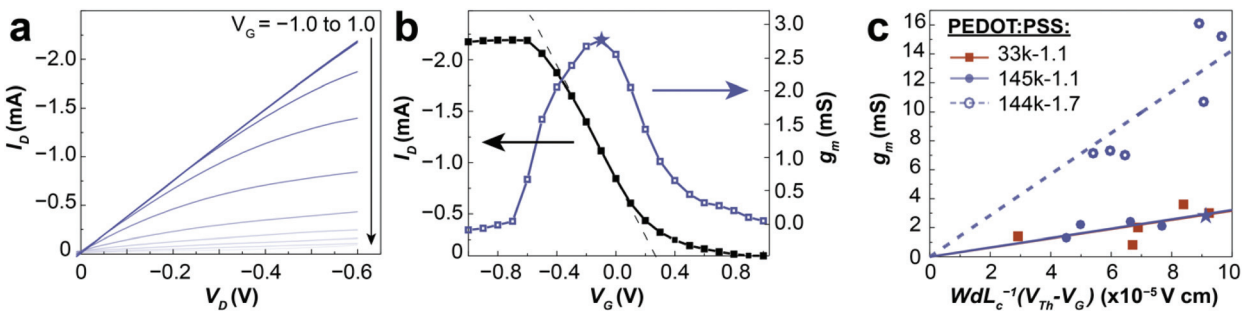

Fig. 5 Performance of PEDOT:PSS samples in OECTs. (a) Output and (b) transfer curves of **PEDOT:PSS 145k-1.1**. (c) Transconductance scaling behaviors of **PEDOT:PSS 33k-1.1**, **PEDOT:PSS 145k-1.1**, and **PEDOT:PSS 144k-1.7**. (The star symbol represents the sample characterized in Fig. 5a and b.)

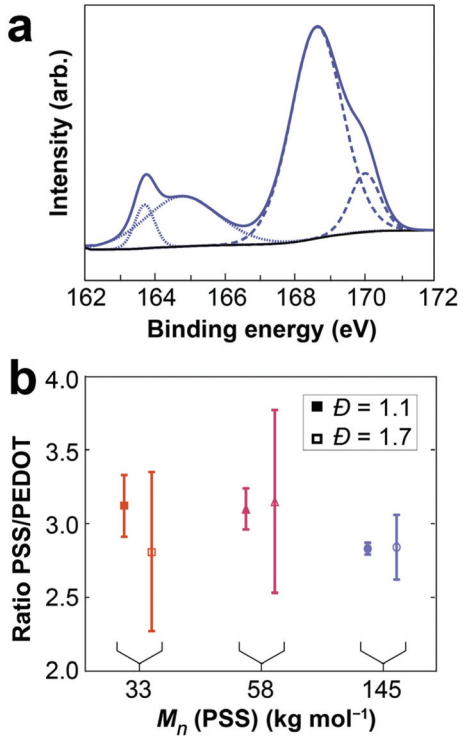

Fig. 6 Analysis of the composition of PEDOT:PSS films. (a) S(2p) XPS spectra of **PEDOT:PSS 145k-1.1** with 5 vol% EG, 1 vol% GOPS, and 0.1 vol% DBSA. The profiles were fitted with two symmetric/asymmetric Gaussian–Lorenzian functions. (b) Ratio of PSS/PEDOT provided by the S(2p) XPS spectra of PEDOT:PSS film with 5 vol% EG, 1 vol% GOPS, and 0.1 vol% DBSA additives, as function of the molecular weight and dispersity of PSS.

with EG, GOPS, and DBSA as these conditions are more relevant to mixed ionic-electronic conduction experiments under aqueous conditions. We found that the PSS/PEDOT ratio barely decreased from 3.12 to 3.10 to 2.83 with increasing molecular weight of PSS (33, 58, and 145 kg mol^{-1}, respectively) at low dispersity. At higher dispersity of PSS, no particular trends could be extracted from the XPS data. The larger error bars for $Đ$ = 1.7 may be indicative of heterogeneities in the PEDOT:PSS films with largely phase separated PEDOT- and PSS-rich domains. These observations are consistent with our abovementioned experiments showing that the conductivity of PEDOT:PSS is weakly dependent on the molecular weight of the PSS but is essentially independent of its dispersity. They are also in agreement with previous reports which show that higher electronic conductivity is obtained at lower ratios of PSS/PEDOT.[64]

To gain more insights into the effect of the molecular weight and size distribution of PSS on the crystallinity and packing of PEDOT:PSS, we performed grazing incidence wide-angle X-ray scattering (GIWAXS) measurements. As seen in the 2-D GIWAXS patterns (Fig. S6†), lamellar stacks were primarily oriented out-of-plane while PSS stacking was largely isotropic. In the 145 kg mol^{-1}samples especially, crystallites with out-of-plane π-stack orientation were predominant. As seen from the linecuts (Fig. S7†), all samples show some peaks at 0.25 Å^{-1} (d = 2.50 nm, lamellar stacking of PEDOT-rich domains twined in PSS),[34,65] 0.6 Å^{-1} (d = 1.05 nm, lamellar structure stacking of PEDOT:PSS),[65] 1.4 Å^{-1} (d = 0.45 nm, PSS amorphous halo),[66] and 1.8 Å^{-1} (d = 0.35 nm, π–π stacking of PEDOT).[67] Though there appeared to be no clear trends in stacking distances with molecular weight, for samples of similar molecular weight, the lamellar spacing decreased for higher $Đ$. Similarly, differences in the π stacking distance are within the margin of error for fitting except for the low $Đ$ 145 kg mol^{-1} sample. The 145k-1.7 sample had a π stack spacing that was ∼ 0.2 Å smaller than that of 145k-1.1 (Table S3†), which could explain the observed difference in mobility between the two samples. GIWAXS alone cannot explain the differences obtained in the OECT measurements. Therefore, atomic force microscopy (AFM) was carried out to characterize the surface morphology of the PEDOT:PSS films without additives (Fig. S8†) and with EG, GOPS and DBSA (Fig. 7).[61] As previously described, the microstructure of PEDOT:PSS consists of PEDOT-rich domains surrounded by PSS-rich regions.[67–69] According to Shen *et al.*, the brighter domains on the AFM phase images (higher phase angle) can be assigned to the PEDOT-rich regions, whereas darker domains correspond to the relatively softer PSS-rich regions.[70] Without additives, all of the samples show PEDOT islands of varying sizes from 20 nm to 45 nm dispersed in PSS (Fig. S8†). With the exception of **PEDOT:PSS 33k-1.1**, which shows some interconnected PEDOT domains, most samples exhibit mainly isolated PEDOT domains which explains the relatively low electronic conductivity of the samples without secondary doping. As expected,[71] the addition of EG, GOPS, and DBSA led to significant changes in the films morphology (Fig. 7) with all samples now exhibiting much more interconnected PEDOT domains. This morphology is consistent with the increase in conductivity observed in the dry films. To calculate the average domain size for the PEDOT domains, we performed a 2D-Fourier transform (2D-FFT) of the AFM phase images and applied a power spectral density (PSD) analysis (Fig. S9 and Table S4†) as previously described.[72,73] We found that higher dispersity of PSS led to larger PEDOT domain sizes (∼32 nm) when compared with low dispersity PSS (∼23 nm). This domain size effect, however, seems largely independent from the molecular weight of the PSS. This observation is in agreement with the OECT measurements, showing that at similar dispersity, [μC^*] is independent of the molecular weight of PSS. The AFM images also confirm data from the XPS showing more heterogeneity in the PEDOT:PSS films at higher dispersity. This difference is particularly visible when comparing the two PEDOT:PSS samples with a high molecular weight, **PEDOT:PSS 145k-1.1** (Fig. 7e) and **PEDOT:PSS 145k-1.7** (Fig. 7f). Both samples exhibit short and irregular elongated features, likely representative of PEDOT domains. But, with high dispersity PSS (Fig. 7f), large patches of interconnected PSS-rich domains (dark) are clearly visible which are largely absent at low dispersity (Fig. 7e). On one hand, this phase separation between ionically-conductive PSS domains and electronically-conductive PEDOT domains (lower interfacial area) is likely responsible for the slightly reduced ionic-electronic

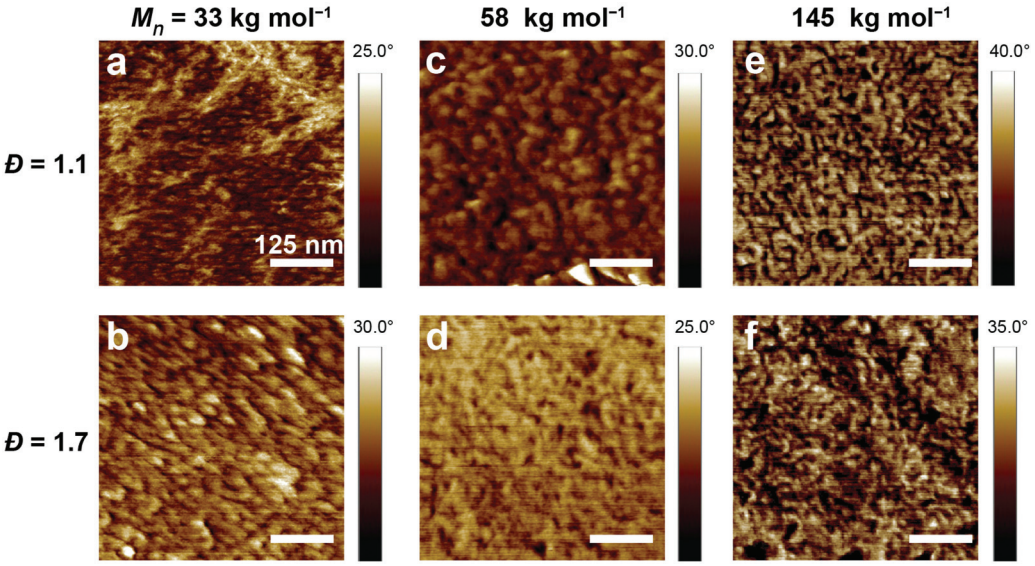

Fig. 7 AFM phase images of PEDOT:PSS thin films with 5 vol% EG, 1 vol% GOPS, and 0.1 vol% DBSA. (a) PEDOT:PSS 33k-1.1; (b) PEDOT:PSS 32k-1.7; (c) PEDOT:PSS 58k-1.1; (d) PEDOT:PSS 58k-1.7; (e) PEDOT:PSS 145k-1.1; and (f) PEDOT:PSS 144k-1.7 (scale bar: 125 nm).

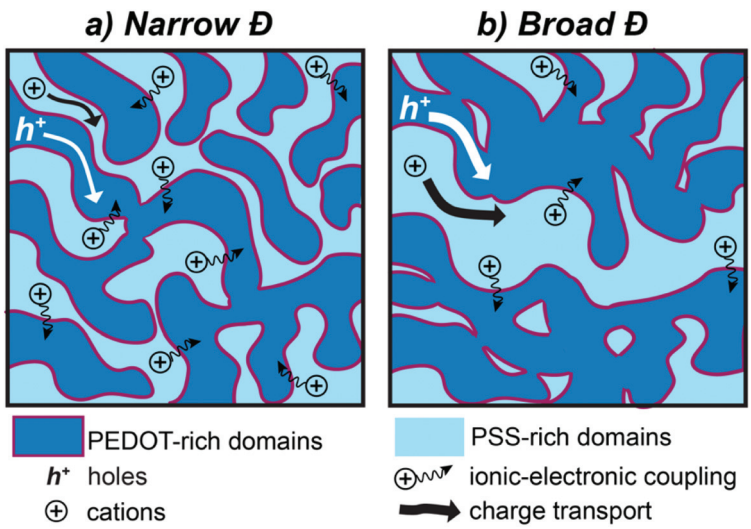

Fig. 8 Schematic of the proposed interpretation for the difference in OECT performance of PEDOT:PSS based on PSS size distribution (*Đ*). (a) PEDOT:PSS with narrow PSS *Đ*. (b) PEDOT:PSS with broad PSS *Đ*. The broad dispersity of PSS leads to larger domain sizes making it easier for holes (white arrow) to transport through the PEDOT-rich domains and cations (black arrow) to transport through the PSS-rich domains. Ionic-electronic coupling (wavy arrows) is lower at broad *Đ* due to a reduction in the interfacial area (in red) between PEDOT- and PSS-rich domains.

coupling observed by CV.[16] On the other hand, it promotes better charge transport during the OECT operation (higher μ_{OECT}). These morphological effects are summarized schematically in Fig. 8. The use of broad dispersity PSS (*Đ* = 1.7) induces an increase in charge mobility in PEDOT:PSS which compensates for the lower ionic-electronic coupling, overall allowing us to achieve higher performance in OECT. We hypothesize that the morphological features in high dispersity PSS samples result from the presence of shorter PSS chains in the blend. These shorter chains are potentially acting as oligomeric plasticizers. During the annealing process, phase separation from larger PSS chains—containing higher loadings of PEDOT—could take place, which leads to the heterogeneous morphology observed. We are currently working on a follow-up study to test this hypothesis by purposefully introducing oligomeric PSS in high molecular weight PEDOT:PSS samples.

Conclusions

Using RAFT polymerization, we have synthesized a series of PSS with varying molecular weights and monomodal size dis-

tributions. These polymers were then used in the synthesis of PEDOT:PSS, which were further characterized for their performance as mixed ionic-electronic conductors. We have demonstrated the importance of considering the molecular weight and size distribution of PSS when interested in the electronic properties of PEDOT:PSS both in the dry state and under aqueous electrochemical conditions. We found that the electrical conductivity in the dry state of PEDOT:PSS is most dependent on the molecular weight of PSS, although the direction of the trend depends on the presence of secondary additives affecting the film morphology. Unlike past reports, we did not find a significant effect of the size distribution on the conductivity when monomodal distributions were maintained for PSS. This finding highlights the importance of precisely controlling the shape of the PSS size distribution when looking at dispersity effects. Conversely, under aqueous electrochemical conditions, dispersity effects dominated over molecular weight. We found that the molecular weight of PSS had little influence on mixed ionic-electronic transport, but increasing the dispersity of PSS led to lower ionic-electronic coupling and higher charge mobility, overall leading to higher performance of PEDOT:PSS in organic electrochemical transistors. The highest mobility-capacitance product [μC^*] obtained was 142 F cm^{-1} V^{-1} s^{-1} for PEDOT:PSS with a molecular weight of 144 kg $mol^{-1}$and dispersity of 1.7, higher than the previously reported value for commercial PEDOT:PSS with the same additives (100 F cm^{-1} V^{-1} s^{-1}).[34] These results demonstrate a promising route towards understanding and optimizing organic mixed ionic-electronic conductors by controlling their size distribution to promote film heterogeneity. Given the widespread use of PEDOT:PSS, we expect these results to inspire new design considerations for mixed conductors with applications in bioelectronics, energy storage, stretchable electronics, and neuromorphic computing.

Author Contributions

C.Y.L., Y.W., E.A., D.M. D.M.N., R.W., B.X., and J.S. collected and analysed the data. L.V.K. conceptualized and supervised the project. J.R. and D.C.M. supervised the GIWAXS and EIS experiments, respectively. C.Y.L. and L.V.K. wrote the original draft, then all the authors contributed to editing the article.

Conflicts of interest

The authors declare no competing financial interest. The content is solely the responsibility of the authors and does not necessarily represent the official views of the National Institutes of Health.

Acknowledgements

Research reported in this publication was supported by National Institute of General Medical Sciences or the National Institutes of Health under Award Number P20GM104316. This research was also supported by start-up funds to L.V.K. from the University of Delaware (UD). E.C.A. would like to thank the Chemistry-Biology Interface Program for his #T32-GM008550 scholarship. The authors thank Dr. Jing Qu for her assistance on GIWAXS and thank the Advanced Materials Characterization Laboratory in the Patrick A. Harker Interdisciplinary Science and Engineering Laboratory (ISE-lab) at the University of Delaware. We acknowledge Dr. Chandran Sabanayagam and the Bio-imaging center at the University of Delaware for AFM assistance. We thank the Surface Analysis Facility for XPS assistance, and UD Nanofabrication facility for the film thickness measurements. J.R., D.M., R.W. acknowledge support from the National Science Foundation (Award No. DMR 1751308) and the Alfred P. Sloan Foundation (Award No. FG-2019-12046). This work used resources of the Advanced Photon Source (beamline 8-ID-E), a U.S. Department of Energy (DOE) Office of Science User Facility operated for the DOE Office of Science by Argonne National Laboratory under Contract No. DE-AC02-06CH11357.

References

1 Y. Cao, G. Yu, C. Zhang, R. Menon and A. J. Heeger, Polymer Light-Emitting Diodes with Polyethylene Dioxythiophene-Polystyrene Sulfonate as the Transparent Anode, *Synth. Met.*, 1997, **87**, 171.
2 L. Groenendaal, F. Jonas, D. Freitag, H. Pielartzik and J. R. Reynolds, Poly(3,4-Ethylenedioxythiophene) and Its Derivatives: Past, Present, and Future, *Adv. Mater.*, 2000, **12**, 481.
3 Y. Wen and J. Xu, Scientific Importance of Water-Processable PEDOT–PSS and Preparation, Challenge and New Application in Sensors of Its Film Electrode: A Review, *J. Polym. Sci., Part A: Polym. Chem.*, 2017, **55**, 1121.
4 F. Jonas and J. T. Morrison, 3,4-Polyethylenedioxythiophene (PEDT): Conductive Coatings Technical Applications and Properties, *Synth. Met.*, 1997, **85**, 1397.
5 G. Greczynski, T. Kugler, M. Keil, W. Osikowicz, M. Fahlman and W. R. Salaneck, Photoelectron Spectroscopy of Thin Films of PEDOT–PSS Conjugated Polymer Blend: A Mini-Review and Some New Results, *J. Electron Spectrosc. Relat. Phenom.*, 2001, **121**, 1.
6 L.-M. Chen, Z. Hong, G. Li and Y. Yang, Recent Progress in Polymer Solar Cells: Manipulation of Polymer:Fullerene Morphology and the Formation of Efficient Inverted Polymer Solar Cells, *Adv. Mater.*, 2009, **21**, 1434.
7 J. Ouyang, "Secondary Doping" Methods to Significantly Enhance the Conductivity of PEDOT:PSS for Its Application as Transparent Electrode of Optoelectronic Devices, *Displays*, 2013, **34**, 423.
8 R. Yue and J. Xu, Poly(3,4-Ethylenedioxythiophene) as Promising Organic Thermoelectric Materials: A Mini-Review, *Synth. Met.*, 2012, **162**, 912.

9 Y. Liang, Z. Tao and J. Chen, Organic Electrode Materials for Rechargeable Lithium Batteries, *Adv. Energy Mater.*, 2012, **2**, 742.
10 G. A. Snook, P. Kao and A. S. Best, Conducting-Polymer-Based Supercapacitor Devices and Electrodes, *J. Power Sources*, 2011, **196**, 1.
11 P. Qibing, Y. Gang, Z. Chi, Y. Yang and H. A. J. Polymer, Light-Emitting Electrochemical Cells, *Science*, 1995, **269**, 1086.
12 Y. Ding, M. A. Invernale and G. A. Sotzing, Conductivity Trends of PEDOT-PSS Impregnated Fabric and the Effect of Conductivity on Electrochromic Textile, *ACS Appl. Mater. Interfaces*, 2010, **2**, 1588.
13 E. Smela, Conjugated Polymer Actuators for Biomedical Applications, *Adv. Mater.*, 2003, **15**, 481.
14 J. Jang, J. Ha and J. Cho, Fabrication of Water-Dispersible Polyaniline-Poly(4-Styrenesulfonate) Nanoparticles for Inkjet-Printed Chemical-Sensor Applications, *Adv. Mater.*, 2007, **19**, 1772.
15 K. A. Ludwig, J. D. Uram, J. Yang, D. C. Martin and D. R. Kipke, Chronic Neural Recordings Using Silicon Microelectrode Arrays Electrochemically Deposited with a Poly(3,4-Ethylenedioxythiophene) (PEDOT) Film, *J. Neural Eng.*, 2006, **3**, 59.
16 B. D. Paulsen, K. Tybrandt, E. Stavrinidou and J. Rivnay, Organic Mixed Ionic–Electronic Conductors, *Nat. Mater.*, 2020, **19**, 13.
17 P. Gkoupidenis, N. Schaefer, B. Garlan and G. G. Malliaras, Neuromorphic Functions in PEDOT:PSS Organic Electrochemical Transistors, *Adv. Mater.*, 2015, **27**, 7176.
18 Y. Van De Burgt, E. Lubberman, E. J. Fuller, S. T. Keene, G. C. Faria, S. Agarwal, M. J. Marinella, A. Alec Talin and A. Salleo, A Non-Volatile Organic Electrochemical Device as a Low-Voltage Artificial Synapse for Neuromorphic Computing, *Nat. Mater.*, 2017, **16**, 414.
19 J. Ouyang, Q. Xu, C.-W. Chu, Y. Yang, G. Li and J. Shinar, On the Mechanism of Conductivity Enhancement in Poly (3,4-Ethylenedioxythiophene):Poly(Styrene Sulfonate) Film through Solvent Treatment, *Polymer*, 2004, **45**, 8443.
20 E. Dauzon, A. E. Mansour, M. R. Niazi, R. Munir, D.-M. Smilgies, X. Sallenave, C. Plesse, F. Goubard and A. Amassian, Conducting and Stretchable PEDOT:PSS Electrodes: Role of Additives on Self-Assembly, Morphology, and Transport, *ACS Appl. Mater. Interfaces*, 2019, **11**, 17570.
21 P. Sakunpongpitiporn, K. Phasuksom, N. Paradee and A. Sirivat, Facile Synthesis of Highly Conductive PEDOT: PSS via Surfactant Templates, *RSC Adv.*, 2019, **9**, 6363.
22 J. Y. Oh, S. Kim, H.-K. Baik and U. Jeong, Conducting Polymer Dough for Deformable Electronics, *Adv. Mater.*, 2016, **28**, 4455.
23 E. Hosseini, V. Ozhukil Kollath and K. Karan, The Key Mechanism of Conductivity in PEDOT:PSS Thin Films Exposed by Anomalous Conduction Behaviour upon Solvent-Doping and Sulfuric Acid Post-Treatment, *J. Mater. Chem. C*, 2020, **8**, 3982.
24 S. Xu, M. Hong, X.-L. Shi, Y. Wang, L. Ge, Y. Bai, L. Wang, M. Dargusch, J. Zou and Z.-G. Chen, High-Performance PEDOT:PSS Flexible Thermoelectric Materials and Their Devices by Triple Post-Treatments, *Chem. Mater.*, 2019, **31**, 5238.
25 A. Hu, L. Tan, X. Hu, L. Hu, Q. Ai, X. Meng, L. Chen and Y. Chen, Crystallization and Conformation Engineering of Solution-Processed Polymer Transparent Electrodes with High Conductivity, *J. Mater. Chem. C*, 2017, **5**, 382.
26 N. A. Shahrim, Z. Ahmad, A. Wong Azman, Y. Fachmi Buys and N. Sarifuddin, Mechanisms for Doped PEDOT:PSS Electrical Conductivity Improvement, *Mater. Adv.*, 2021, **2**, 7118.
27 D. McGillivray, J. P. Thomas, M. Abd-Ellah, N. F. Heinig and K. T. Leung, Performance Enhancement by Secondary Doping in PEDOT:PSS/Planar-Si Hybrid Solar Cells, *ACS Appl. Mater. Interfaces*, 2016, **8**, 34303.
28 H. Shi, C. Liu, Q. Jiang and J. Xu, Effective Approaches to Improve the Electrical Conductivity of PEDOT:PSS: A Review, *Adv. Electron. Mater.*, 2015, **1**, 1500017.
29 M. N. Gueye, A. Carella, J. Faure-Vincent, R. Demadrille and J.-P. Simonato, Progress in Understanding Structure and Transport Properties of PEDOT-Based Materials: A Critical Review, *Prog. Mater. Sci.*, 2020, **108**, 100616.
30 D. Ju, D. Kim, H. Yook, J. W. Han and K. Cho, Controlling Electrostatic Interaction in PEDOT:PSS to Overcome Thermoelectric Tradeoff Relation, *Adv. Funct. Mater.*, 2019, **29**, 1905590.
31 Z. Fan, D. Du, H. Yao and J. Ouyang, Higher PEDOT Molecular Weight Giving Rise to Higher Thermoelectric Property of PEDOT:PSS: A Comparative Study of Clevios P and Clevios PH1000, *ACS Appl. Mater. Interfaces*, 2017, **9**, 11732.
32 J. Kim, C. Park, S. Im, H. Lee and J. H. Kim, Effect of Molecular Weight Distribution of PSSA on Electrical Conductivity of PEDOT:PSS, *RSC Adv.*, 2019, **9**, 4028.
33 J. Rivnay, S. Inal, B. A. Collins, M. Sessolo, E. Stavrinidou, X. Strakosas, C. Tassone, D. M. Delongchamp and G. G. Malliaras, Structural Control of Mixed Ionic and Electronic Transport in Conducting Polymers, *Nat. Commun.*, 2016, **7**, 11287.
34 S.-M. Kim, C.-H. Kim, Y. Kim, N. Kim, W.-J. Lee, E.-H. Lee, D. Kim, S. Park, K. Lee, J. Rivnay and M.-H. Yoon, Influence of PEDOT:PSS Crystallinity and Composition on Electrochemical Transistor Performance and Long-Term Stability, *Nat. Commun.*, 2018, **9**, 3858.
35 D. Mantione, I. del Agua, W. Schaafsma, M. ElMahmoudy, I. Uguz, A. Sanchez-Sanchez, H. Sardon, B. Castro, G. G. Malliaras and D. Mecerreyes, Low-Temperature Cross-Linking of PEDOT:PSS Films Using Divinylsulfone, *ACS Appl. Mater. Interfaces*, 2017, **9**, 18254.
36 R. Whitfield, K. Parkatzidis, N. P. Truong, T. Junkers and A. Anastasaki, Tailoring Polymer Dispersity by RAFT Polymerization: A Versatile Approach, *Chem*, 2020, **6**, 1340.
37 Z. Wang, J. Yan, T. Liu, Q. Wei, S. Li, M. Olszewski, J. Wu, J. Sobieski, M. Fantin, M. R. Bockstaller and

K. Matyjaszewski, Control of Dispersity and Grafting Density of Particle Brushes by Variation of ATRP Catalyst Concentration, *ACS Macro Lett.*, 2019, **8**, 859.

38 M. Rolland, N. P. Truong, R. Whitfield and A. Anastasaki, Tailoring Polymer Dispersity in Photoinduced Iron-Catalyzed ATRP, *ACS Macro Lett.*, 2020, **9**, 459.

39 L. A. Camacho-Cruz, M. A. Velazco-Medel and E. Bucio, Aqueous Polymerizations, *Green Sustainable Process for Chemical and Environmental Engineering and Science: Organic Synthesis in Water and Supercritical Water*, 2020, p. 275.

40 D. T. Gentekos, R. J. Sifri and B. P. Fors, Controlling Polymer Properties through the Shape of the Molecular-Weight Distribution, *Nat. Rev. Mater.*, 2019, **4**, 761.

41 C. V. L. Keef, V. Kayser, S. Tronboll, C. W. Carpenter, N. B. Root, M. Finn III, T. F. O'Connor, S. N. Abuhamdieh, D. M. Davies, R. Runser, Y. S. Meng, V. S. Ramachandran and D. J. Lipomi, Virtual Texture Generated Using Elastomeric Conductive Block Copolymer in a Wireless Multimodal Haptic Glove, *Adv. Intell. Syst.*, 2020, **2**, 2000018.

42 S. Perrier, 50th Anniversary Perspective: RAFT Polymerization—A User Guide, *Macromolecules*, 2017, **50**, 7433.

43 A. Håkansson, S. Han, S. Wang, J. Lu, S. Braun, M. Fahlman, M. Berggren, X. Crispin and S. Fabiano, Effect of (3-Glycidyloxypropyl)Trimethoxysilane (GOPS) on the Electrical Properties of PEDOT:PSS Films, *J. Polym. Sci., Part B: Polym. Phys.*, 2017, **55**, 814.

44 A. Savva, S. Wustoni and S. Inal, Ionic-to-Electronic Coupling Efficiency in PEDOT:PSS Films Operated in Aqueous Electrolytes, *J. Mater. Chem. C*, 2018, **6**, 12023.

45 N. Matsuhisa, Y. Jiang, Z. Liu, G. Chen, C. Wan, Y. Kim, J. Kang, H. Tran, H.-C. Wu, I. You, Z. Bao and X. Chen, High-Transconductance Stretchable Transistors Achieved by Controlled Gold Microcrack Morphology, *Adv. Electron. Mater.*, 2019, **5**, 1900347.

46 H. Y. Du, X. X. Liu, Z. Ren and P. P. Liu, Capacitance Characteristic of PEDOT Electrodeposited on Different Substrates, *J. Solid State Electrochem.*, 2018, **22**, 3947.

47 M. Bianchi, S. Carli, M. Di Lauro, M. Prato, M. Murgia, L. Fadiga and F. Biscarini, Scaling of Capacitance of PEDOT:PSS: Volume vs. Area, *J. Mater. Chem. C*, 2020, **8**, 11252.

48 Y. Xu, S. Pei, Y. Yan, L. Wang, G. Xu, S. Yarlagadda and T.-W. Chou, High-Performance Structural Supercapacitors Based on Aligned Discontinuous Carbon Fiber Electrodes and Solid Polymer Electrolytes, *ACS Appl. Mater. Interfaces*, 2021, **13**, 11774.

49 J. Rivnay, P. Leleux, M. Ferro, M. Sessolo, A. Williamson, D. A. Koutsouras, D. Khodagholy, M. Ramuz, X. Strakosas, R. M. Owens, C. Benar, J.-M. Badier, C. Bernard and G. G. Malliaras, High-Performance Transistors for Bioelectronics through Tuning of Channel Thickness, *Sci. Adv.*, 2015, **1**, e1400251.

50 D. A. Koutsouras, P. Gkoupidenis, C. Stolz, V. Subramanian, G. G. Malliaras and D. C. Martin, Impedance Spectroscopy of Spin-Cast and Electrochemically Deposited PEDOT:PSS Films on Microfabricated Electrodes with Various Areas, *ChemElectroChem*, 2017, **4**, 2321.

51 P. D. Jones, A. Moskalyuk, C. Barthold, K. Gutöhrlein, G. Heusel, B. Schröppel, R. Samba and M. Giugliano, Low-Impedance 3D PEDOT:PSS Ultramicroelectrodes, *Front. Neurosci.*, 2020, **14**, 405.

52 S. Nagane, P. Sitarik, Y. Wu, Q. Baugh, S. Chhatre, J. Lee and D. C. Martin, Functionalized Polythiophene Copolymers for Electronic Biomedical Devices, *MRS Adv.*, 2020, **5**, 943.

53 N. A. B. Ismail, F. Abd-Wahab and W. W. A. W. Salim, Cyclic Voltammetry and Electrochemical Impedance Spectroscopy of Partially Reduced Graphene Oxide - PEDOT:PSS Transducer for Biochemical Sensing, *IEEE-EMBS Conf. Biomed. Eng. Sci. (IECBES)*, 2018, 330.

54 F. Sundfors, J. Bobacka, A. Ivaska and A. Lewenstam, Kinetics of Electron Transfer between Fe(CN)63−/4− and Poly(3,4-Ethylenedioxythiophene) Studied by Electrochemical Impedance Spectroscopy, *Electrochim. Acta*, 2002, **47**, 2245.

55 J. Bobacka, A. Lewenstam and A. Ivaska, Electrochemical Impedance Spectroscopy of Oxidized Poly(3,4-Ethylenedioxythiophene) Film Electrodes in Aqueous Solutions, *J. Electroanal. Chem.*, 2000, **489**, 17.

56 E. Stavrinidou, M. Sessolo, B. Winther-Jensen, S. Sanaur and G. G. Malliaras, A Physical Interpretation of Impedance at Conducting Polymer/Electrolyte Junctions, *AIP Adv.*, 2014, **4**, 17127.

57 D. Khodagholy, J. Rivnay, M. Sessolo, M. Gurfinkel, P. Leleux, L. H. Jimison, E. Stavrinidou, T. Herve, S. Sanaur, R. M. Owens and G. G. Malliaras, High Transconductance Organic Electrochemical Transistors, *Nat. Commun.*, 2013, **4**, 2133.

58 M. J. Donahue, A. Williamson, X. Strakosas, J. T. Friedlein, R. R. McLeod, H. Gleskova and G. G. Malliaras, High-Performance Vertical Organic Electrochemical Transistors, *Adv. Mater.*, 2018, **30**, 1705031.

59 D. A. Bernards and G. G. Malliaras, Steady-State and Transient Behavior of Organic Electrochemical Transistors, *Adv. Funct. Mater.*, 2007, **17**, 3538.

60 S. Inal, G. G. Malliaras and J. Rivnay, Benchmarking Organic Mixed Conductors for Transistors, *Nat. Commun.*, 2017, **8**, 1767.

61 X. Crispin, F. L. E. Jakobsson, A. Crispin, P. C. M. Grim, P. Andersson, A. Volodin, C. van Haesendonck, M. Van der Auweraer, W. R. Salaneck and M. Berggren, The Origin of the High Conductivity of Poly(3,4-Ethylenedioxythiophene)–Poly(Styrenesulfonate) (PEDOT–PSS) Plastic Electrodes, *Chem. Mater.*, 2006, **18**, 4354.

62 X. Crispin, S. Marciniak, W. Osikowicz, G. Zotti, A. W. D. van der Gon, F. Louwet, M. Fahlman, L. Groenendaal, F. De Schryver and W. R. Salaneck, Conductivity, Morphology, Interfacial Chemistry, and

Stability of Poly(3,4-Ethylene Dioxythiophene)–Poly(Styrene Sulfonate): A Photoelectron Spectroscopy Study, *J. Polym. Sci., Part B: Polym. Phys.*, 2003, **41**, 2561.

63 D. Alemu, H.-Y. Wei, K.-C. Ho and C.-W. Chu, Highly Conductive PEDOT:PSS Electrode by Simple Film Treatment with Methanol for ITO-Free Polymer Solar Cells, *Energy Environ. Sci.*, 2012, **5**, 9662.

64 G. Zotti, S. Zecchin, G. Schiavon, F. Louwet, L. Groenendaal, X. Crispin, W. Osikowicz, W. Salaneck and M. Fahlman, Electrochemical and XPS Studies toward the Role of Monomeric and Polymeric Sulfonate Counterions in the Synthesis, Composition, and Properties of Poly(3,4-Ethylenedioxythiophene), *Macromolecules*, 2003, **36**, 3337.

65 K. Itoh, Y. Kato, Y. Honma, H. Masunaga, A. Fujiwara, S. Iguchi and T. Sasaki, Structural Alternation Correlated to the Conductivity Enhancement of PEDOT:PSS Films by Secondary Doping, *J. Phys. Chem. C*, 2019, **123**, 13467.

66 Q. Wei, M. Mukaida, Y. Naitoh and T. Ishida, Morphological Change and Mobility Enhancement in PEDOT:PSS by Adding Co-Solvents, *Adv. Mater.*, 2013, **25**, 2831.

67 T. Takano, H. Masunaga, A. Fujiwara, H. Okuzaki and T. Sasaki, PEDOT Nanocrystal in Highly Conductive PEDOT:PSS Polymer Films, *Macromolecules*, 2012, **45**, 3859.

68 U. Lang, E. Müller, N. Naujoks and J. Dual, Microscopical Investigations of PEDOT:PSS Thin Films, *Adv. Funct. Mater.*, 2009, **19**, 1215.

69 A. M. Nardes, M. Kemerink, R. A. J. Janssen, J. A. M. Bastiaansen, N. M. M. Kiggen, B. M. W. Langeveld, A. J. J. M. van Breemen and M. M. de Kok, Microscopic Understanding of the Anisotropic Conductivity of PEDOT:PSS Thin Films, *Adv. Mater.*, 2007, **19**, 1196.

70 Y. Wang, R. Song, Y. Li and J. Shen, Understanding Tapping-Mode Atomic Force Microscopy Data on the Surface of Soft Block Copolymers, *Surf. Sci.*, 2003, **530**, 136.

71 T. Horii, Y. Li, Y. Mori and H. Okuzaki, Correlation between the Hierarchical Structure and Electrical Conductivity of PEDOT/PSS, *Polym. J.*, 2015, **47**, 695.

72 X. Cui, J. F. Hetke, J. A. Wiler, D. J. Anderson and D. C. Martin, Electrochemical Deposition and Characterization of Conducting Polymer Polypyrrole/PSS on Multichannel Neural Probes, *Sensors Actuators A Phys.*, 2001, **93**, 8.

73 F. M. Mwema, E. T. Akinlabi and O. P. Oladijo, Dependence of Fractal Characteristics on the Scan Size of Atomic Force Microscopy (AFM) Phase Imaging of Aluminum Thin Films, *Mater. Today Proc.*, 2020, **26**, 1540.